Anelastic AVO approximations continued

Kris Innanen

ABSTRACT

We write down linearized anelastic AVO approximations appropriate for problems involving both elastic and anelastic incidence media. Variations in the anelastic properties of the Earth across the reflecting boundary are expressed in terms of reflectivity- and relative change-type quantities. $R_{\rm PP}$, $R_{\rm PS}$ and $R_{\rm SS}$ coefficients are each investigated. There is a wide range of degrees of accuracy produced by this set of formulas and no obvious pattern. We conclude it is best to have all of the forms "on hand" to fit anelastic AVO situations as they arise.

INTRODUCTION

In recent years there has been an increase in reports of anelastic, as opposed to elastic, seismic AVO behaviour (Chapman et al., 2006; Odebeatu et al., 2006; Quintal et al., 2009; Lines et al., 2012). Since seismic Q is an indicator of fluid content, there is little doubt that extra geophysical and geological information is contained in such signatures. Innanen (2011) has suggested that given this trend, the production of interpretable mathematical forms for anelastic AVO (or AVF, as the case may be), akin to the Aki-Richards and related elastic approximations (e.g., Castagna and Backus, 1993; Foster et al., 2010), is a research priority. In that work anelastic P-P and P-S forms proper to elastic incidence media and anelastic target media were derived. Here we extend that work to include P-P, P-S, and S-S approximations proper to both elastic and anelastic incidence media, and express those approximations both in terms of relative changes of anelastic properties across the reflecting boundary, and reflectivity quantities. We focus exclusively on forward modelling, and linearized forms, whereas Innanen (2011) derived linear and nonlinear formulas for both modelling and inversion.

The formulation for anelastic incidence media is similar to that by which the "elastic incidence" problems discussed above have been generated. The main difference lies in changes to the standard quantities of AVO theory arising from complex incidence medium propagation constants. This complexity extends to all plane-wave AVO quantities we normally discuss: incidence and transmitted angles, V_P/V_S ratios, etc. Since AVO is still *measured* over real variables (x, t, k_x, ω etc.), we have to come to some decisions about how to parametrize the problem: how to map between the complex variables by which the wave interacts with the Earth (in our mathematical models) and the real variables associated with the experiment. Here we arrange all AVO formulas such that the angles on the left hand sides are real, and chosen as if the incidence media were elastic, whereas the angles on the right hand sides are complex and expressive of the anelastic wave propagation model. The two sets of angles map straightforwardly from one to the other.

There are five basic components of this paper. The first part, which appears after the introduction, is a summary of the theory by which linearized anelastic AVO approximations are derived, along with six formulas, the "core" AVO formulas for $R_{\rm PP}$, $R_{\rm PS}$ and $R_{\rm SS}$ given

Symbol	Meaning
V_{P_0}, V_{P_1}	P-wave velocities in incidence and target media
V_{S_0}, V_{S_1}	S-wave velocities in incidence and target media
ρ_0, ρ_1	Densities in incidence and target media
Q_{P_0}, Q_{P_1}	P-wave quality factors in incidence and target media
Q_{S_0}, Q_{S_1}	S-wave quality in incidence and target media
ω	Temporal angular frequency
k_x	Lateral wavenumber
$F_P(\omega)$, $F_S(\omega)$	P- and S-wave attenuation/dispersion coefficients
k_{P_0}, k_{P_1}	P-wave propagation constants
k_{S_0}, k_{S_1}	S-wave propagation constants
R^A_{PP}, R^A_{PS}, R^A_{SP}, R^A_{SS}	Displacement reflection strengths, anelastic incidence media
R^E_{PP}, R^E_{PS}, R^E_{SP}, R^E_{SS}	Displacement reflection strengths, elastic incidence media
R^{EE}_{PP}, R^{EE}_{PS}, R^{EE}_{SP}, R^{EE}_{SS}	Displacement reflection strengths, elastic incidence/target media
A, B, C, D, E, F	Anelastic parameter ratios
γ_A	Anelastic V_P/V_S ratio
a_{VP}, a_{VS}, a_ρ	Elastic perturbations across reflecting boundary
a_{QP}, a_{QS}	Anelastic perturbations across reflecting boundary
θ, ϕ	Elastic angles of incidence for P-, S-waves
θ_A, ϕ_A	Anelastic angles of incidence for P-, S-waves
Γ_i, Γ^i	Functions of angle in the Zoeppritz equations
$\Delta V_P/V_P$, $\Delta V_S/V_S$, $\Delta\rho/\rho$	Elastic relative change/reflectivity quantities
$\Delta Q_P/Q_P$, $\Delta Q_S/Q_S$	Anelastic relative change/reflectivity quantities

Table 1. Table of symbols.

first anelastic and then elastic incidence media. In the second through fifth components of the paper, we re-write the core formulas four times, for each combination of two forms of the relative change in properties, and elastic vs. anelastic incidence media. We illustrate each formula with a numerical example, and summarize the relative accuracy of each in our conclusions.

Symbols used in this paper

In this paper a range of symbols are used repeatedly. To keep these quantities in order, in Table 1 we list the main symbols and their significance.

Parameters for the numerical examples in this paper

To illustrate the numerical character of these formulas, we choose a set of representative elastic and/or anelastic incidence and target medium properties, and compare the exact reflection coefficients with (1) our linear-approximate forms, and (2) the reflection coefficients in the elastic limit, i.e., as if inelasticity had been ignored. The latter will therefore measure the importance to AVO of correctly including anelasticity when it appears. In every numerical case we will calculate an AVO curve at a fixed frequency of $\omega = 2\pi$ rad $\times$10Hz, using reference frequencies of $\omega_P = 2\pi$ rad $\times$120Hz, and $\omega_S = 2\pi$rad $\times$ 60Hz.

Figure number	V_{P_0} (m/s)	V_{S_0} (m/s)	ρ_0 (gm/cc)	Q_{P_0}	Q_{S_0}	V_{P_1} (m/s)	V_{S_1} (m/s)	ρ_1 (gm/cc)	Q_{P_1}	Q_{S_1}
3	2000	1500	2.0	20	15	2500	1600	2.25	10	5
4	2000	1500	2.0	20	15	2500	1600	2.25	15	10
5	2000	1500	2.0	20	15	2500	1700	2.25	10	5
6	2000	1500	2.0	20	15	2500	1600	2.25	10	5
7	2000	1500	2.0	20	15	2500	1600	2.25	15	10
8	2000	1500	2.0	30	25	2500	1700	2.25	15	10
9	2000	1500	2.0	∞	∞	2300	1600	2.25	10	5
10	2000	1500	2.0	∞	∞	2500	1600	2.5	10	5
11	2000	1500	2.0	∞	∞	2200	1550	2.25	10	5
12	2000	1500	2.0	∞	∞	2500	1600	2.5	10	5
13	2000	1500	2.0	∞	∞	2500	1600	2.5	10	5
14	2000	1500	2.0	∞	∞	2500	1600	2.5	10	5

Table 2. Table of elastic/anelastic parameters used in numerical examples. In the left column are the Figure numbers wherein AVO curves are plotted. In the columns to the right are the anelastic medium properties used in those AVO curve calculations.

Our goal is to maintain a more or less constant anelastic model throughout, to aid us in making qualitative comparisons, but we occasionally vary parameters as a reassurance that the model does not involve "special" parameters for which the formulas act in a desirable way. The elastic and/or anelastic parameters used in all the forthcoming examples, along with the relevant figure numbers, are listed in Table 2.

ANELASTIC ZOEPPRITZ EQUATIONS AND LINEARIZED SOLUTIONS

We will treat the anelastic AVO problem in two distinct cases. In case one the incidence medium is elastic (Figure 1a); in case two the incidence medium is anelastic (Figure 1b). We will treat them in reverse order, since once the anelastic incidence medium case is developed the elastic incidence medium case follows with only a few slight changes.

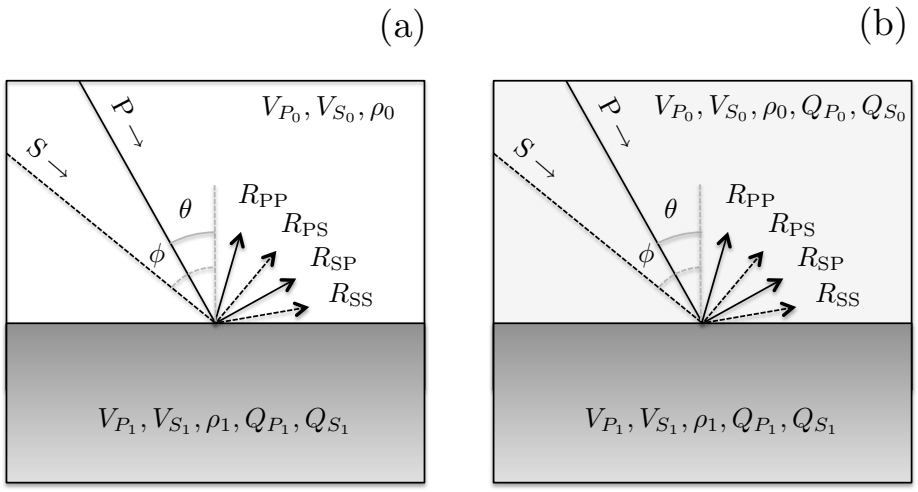

FIG. 1. Anelastic AVO configurations: (a) elastic incidence medium; (b) anelastic incidence medium.

Anelastic incidence medium

We consider an incidence medium in with anelastic parameters V_{P_0}, V_{S_0}, ρ_0, Q_{P_0} and Q_{S_0}, and a target medium with anelastic parameters V_{P_1}, V_{S_1}, ρ_1, Q_{P_1} and Q_{S_1}. The attenuation model is chosen following Aki and Richards (2002), such that the plane P-waves and S-waves have propagation constants

$$\begin{aligned} k_{P_0} &= \frac{\omega}{V_{P_0}}\left[1+Q_{P_0}^{-1}F_P(\omega)\right], \quad k_{S_0} = \frac{\omega}{V_{S_0}}\left[1+Q_{S_0}^{-1}F_S(\omega)\right], \\ k_{P_1} &= \frac{\omega}{V_{P_1}}\left[1+Q_{P_1}^{-1}F_P(\omega)\right], \quad k_{S_1} = \frac{\omega}{V_{S_1}}\left[1+Q_{S_1}^{-1}F_S(\omega)\right], \end{aligned} \tag{1}$$

where

$$\begin{aligned} F_P(\omega) &= \frac{i}{2} - \frac{1}{\pi}\log\left(\frac{\omega}{\omega_P}\right), \\ F_S(\omega) &= \frac{i}{2} - \frac{1}{\pi}\log\left(\frac{\omega}{\omega_S}\right), \end{aligned} \tag{2}$$

and ω_P and ω_S are reference frequencies. If a plane P-wave is incident at the complex angle θ, or a plane S-wave is incident at the complex angle ϕ, and $X = \sin\theta$ and $Y = \sin\phi$, the Zoeppritz equations in matrix form (expressed similarly to the elastic case as by, e.g., Innanen, 2012) are

$$\mathbf{P}\begin{bmatrix} R^A_{\text{PP}} \\ R^A_{\text{PS}} \\ T^A_{\text{PP}} \\ T^A_{\text{PS}} \end{bmatrix} = \mathbf{b}_P, \quad \text{and} \quad \mathbf{S}\begin{bmatrix} R^A_{\text{SS}} \\ R^A_{\text{SP}} \\ T^A_{\text{SS}} \\ T^A_{\text{SP}} \end{bmatrix} = \mathbf{b}_S, \tag{3}$$

where

$$\mathbf{P} = \begin{bmatrix} -X & -\Gamma_B(X) & CX & \Gamma_D(X) \\ \Gamma_1(X) & -BX & \Gamma_C(X) & -DX \\ 2B^2X\Gamma_1(X) & B\Gamma^B(X) & 2AD^2X\Gamma_C(X) & AD\Gamma^D(X) \\ -\Gamma^B(X) & 2B^2X\Gamma_B(X) & 2AC\Gamma^D(X) & -2AD^2X\Gamma_D(X) \end{bmatrix}, \tag{4}$$

$$\mathbf{S} = \begin{bmatrix} Y & -\Gamma_{B^{-1}}(Y) & FY & -\Gamma_E(Y) \\ -\Gamma_1(Y) & -B^{-1}Y & \Gamma_F(Y) & EY \\ -2Y\Gamma_1(Y) & B^{-1}\Gamma^1(Y) & 2AF^2Y\Gamma_F(Y) & -AE\Gamma^F(Y) \\ \Gamma^1(Y) & 2Y\Gamma_{B^{-1}}(Y) & AF\Gamma^F(Y) & 2AF^2Y\Gamma_E(Y) \end{bmatrix}, \tag{5}$$

and

$$\mathbf{b}_P = \begin{bmatrix} X \\ \Gamma_1(X) \\ 2B^2X\Gamma_1(X) \\ \Gamma^B(X) \end{bmatrix}, \quad \text{and} \quad \mathbf{b}_S = \begin{bmatrix} Y \\ \Gamma_1(Y) \\ 2Y\Gamma_1(Y) \\ \Gamma_1(Y) \end{bmatrix}, \tag{6}$$

and where we have used the ratios

$$A = \frac{\rho_1}{\rho_0}, \quad B = \frac{V_{S_0}}{V_{P_0}}\frac{\left[1+Q_{P_0}^{-1}F_P(\omega)\right]}{\left[1+Q_{S_0}^{-1}F_S(\omega)\right]}, \quad C = \frac{V_{P_1}}{V_{P_0}}\frac{\left[1+Q_{P_0}^{-1}F_P(\omega)\right]}{\left[1+Q_{P_1}^{-1}F_P(\omega)\right]} \tag{7}$$

and

$$F = \frac{V_{S_1}}{V_{S_0}} \frac{[1 + Q_{S_0}^{-1} F_S(\omega)]}{[1 + Q_{S_1}^{-1} F_S(\omega)]}, \quad D = BF, \quad E = B^{-1}C \tag{8}$$

and the functions

$$\begin{aligned} \Gamma_j(Z) &= \sqrt{1 - j^2 Z^2}, \\ \Gamma^j(Z) &= 1 - 2j^2 Z^2. \end{aligned} \tag{9}$$

By forming auxiliary matrices $\mathbf{P}_P$, $\mathbf{P}_S$ and $\mathbf{S}_S$, $\mathbf{S}_P$ by replacing the first and second columns of $\mathbf{P}$ and $\mathbf{S}$ with the right hand vectors $\mathbf{b}_P$ and $\mathbf{b}_S$ respectively, we may form exact solutions

$$R_{\text{PP}}^A = \frac{\det\mathbf{P}_P}{\det\mathbf{P}}, \quad R_{\text{PS}}^A = \frac{\det\mathbf{P}_S}{\det\mathbf{P}}, \quad R_{\text{SS}}^A = \frac{\det\mathbf{S}_S}{\det\mathbf{S}}, \quad R_{\text{SP}}^A = \frac{\det\mathbf{S}_P}{\det\mathbf{S}}. \tag{10}$$

For reference, we will call the equivalent elastic reflection coefficients (i.e., obtained by setting $Q_{P_0}^{-1}$ and $Q_{S_0}^{-1} = 0$) by the names R_{PP}^{EE}, R_{PS}^{EE}, R_{SP}^{EE}, and R_{SS}^{EE}. We next define perturbations

$$\begin{aligned} &a_{VP} = 1 - \left(\frac{V_{P_0}}{V_{P_1}}\right)^2, \quad a_{VS} = 1 - \left(\frac{V_{S_0}}{V_{S_1}}\right)^2, \quad a_\rho = 1 - \frac{\rho_0}{\rho_1}, \\ &a_{QP} = 1 - \frac{Q_{P_0}}{Q_{P_1}}, \quad \text{and} \quad a_{QS} = 1 - \frac{Q_{S_0}}{Q_{S_1}}. \end{aligned} \tag{11}$$

For small values of these perturbations and for small angles, we may make the following replacements within the exact equations above:

$$\begin{aligned} \Gamma_j(Z) &\approx 1 - \frac{1}{2} j^2 Z^2, \\ C &\approx 1 + \frac{1}{2} a_{VP} + Q_{P_0}^{-1} F_P(\omega) a_{QP} \\ F &\approx 1 + \frac{1}{2} a_{VS} + Q_{S_0}^{-1} F_S(\omega) a_{QS}. \end{aligned} \tag{12}$$

We substitute equations (7)–(8) with the alterations in equation (12) into the matrices $\mathbf{P}$ and $\mathbf{S}$, form the auxiliary matrices, and calculate the determinants. Assembling terms in $\det\mathbf{P}_P$ that are (a) linear in the perturbations and (b) up to second order in $\sin\theta$ or $\sin\phi$ into $\det\mathbf{P}_P^{(1)}$, and the terms in $\det\mathbf{P}$ that are (a) zeroth order in the perturbations and (b) up to second order in $\sin\theta$ or $\sin\phi$ into $\det\mathbf{P}^{(0)}$, we form linear approximations

$$R_{\text{PP}}^A \approx \frac{\det\mathbf{P}_P^{(1)}}{\det\mathbf{P}^{(0)}}, \quad R_{\text{PS}}^A \approx \frac{\det\mathbf{P}_S^{(1)}}{\det\mathbf{P}^{(0)}}, \quad R_{\text{SS}}^A \approx \frac{\det\mathbf{S}_S^{(1)}}{\det\mathbf{S}^{(0)}}, \tag{13}$$

neglecting R_{SP}. The superscript A refers to the anelasticity of the incidence medium.

To write these approximations out explicitly we need first to come to grips with the complexity of the P- and S-wave angles of incidence θ and ϕ. We will proceed as follows.

In Figure 2 the plane wave geometry connecting propagation constants (which appear as the hypotenuses of the right triangles) to the incidence angles and horizontal wavenumbers are illustrated. In Figures 2a-b the anelastic case is considered. Evidently

$$\begin{aligned} \sin\theta_A &= \frac{V_{P_0}k_x}{\omega}\left[1+Q_{P_0}^{-1}F_P(\omega)\right]^{-1} \\ \sin\phi_A &= \frac{V_{S_0}k_x}{\omega}\left[1+Q_{S_0}^{-1}F_S(\omega)\right]^{-1} \end{aligned} \tag{14}$$

holds. In the elastic limit, as illustrated in Figures 2c-d, we have rather that

$$\begin{aligned} \sin\theta &= \frac{V_{P_0}k_x}{\omega} \\ \sin\phi &= \frac{V_{S_0}k_x}{\omega}; \end{aligned} \tag{15}$$

combining equations (14) and (15) we can map between (θ_A, ϕ_A) and (θ, ϕ) straightforwardly via

$$\begin{aligned} \sin\theta_A &= \sin\theta\left[1+Q_{P_0}^{-1}F_P(\omega)\right]^{-1} \\ \sin\phi_A &= \sin\phi\left[1+Q_{S_0}^{-1}F_S(\omega)\right]^{-1}. \end{aligned} \tag{16}$$

The most convenient parametrization of the AVO curves will be to use θ and ϕ, which are real-valued and closely related to experimental variables, as output variables (i.e., on the left-hand side of the AVO formulas), and to use θ_A and ϕ_A, which are complex and closely related to anelastic wave propagation variables, as input variables (i.e., on the right-hand side of the AVO formulas).

We use equation (16) to map from the real output variables θ and ω to the complex input angles θ_A and ϕ_A to express the linearizations. We may also, at this point in the derivation, decide to replace the right-hand side angles θ_A and ϕ_A, which are formally the angles of incidence, with the average of the incidence angles and transmission angles (as first empirically suggested by Shuey, 1985). The decision to do this, or not do it, in practice will be based on the type of information we feel is available. The results to follow in this paper can be explored with or without this replacement; we will examine them with the replacement, i.e., using average angles.

The core approximations for an anelastic incidence medium are, then,

$$\begin{aligned} R^A_{\mathrm{PP}}(\theta,\omega) \approx & \frac{1}{4}(1+\tan^2\theta_A)a_{VP} + \frac{1}{2}\left[1-4\left(\frac{1}{\gamma_A}\right)^2\sin^2\theta_A\right]a_\rho \\ & -2\left(\frac{1}{\gamma_A}\right)^2\sin^2\theta_A a_{VS} + \frac{1}{2}Q_{P_0}^{-1}F_P(\omega)\left(1+\tan^2\theta_A\right)a_{QP} \\ & -4\left(\frac{1}{\gamma_A}\right)^2 Q_{S_0}^{-1}F_S(\omega)\sin^2\theta_A a_{QS}, \end{aligned} \tag{17}$$

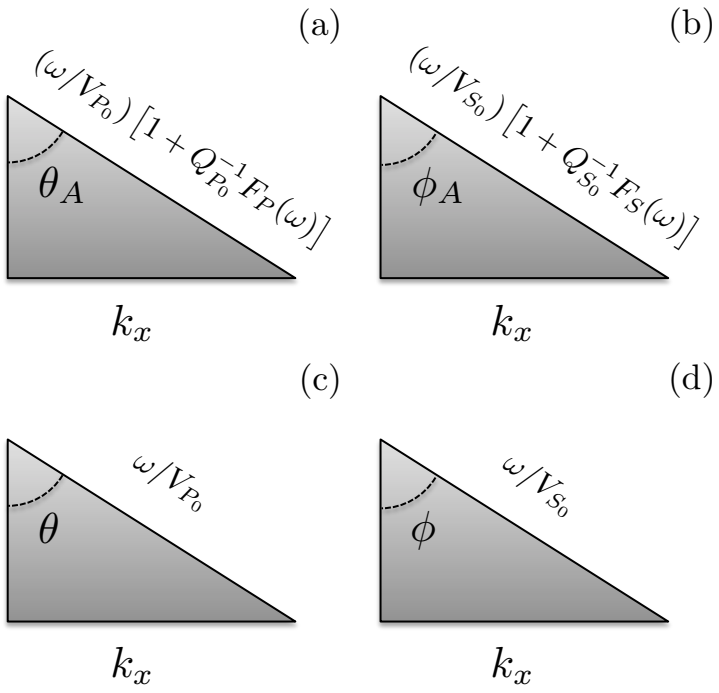

FIG. 2. Parametrizing reflection strengths when angles are complex. (a)–(b) Plane wave geometry for anelastic incidence media. (c)–(d) Plane wave geometry for elastic incidence media.

for P-P reflection strengths (using the common replacement $\sin\theta_A \approx \tan\theta_A$ for the P-wave velocity term),

$$\begin{aligned} R^A_{\rm PS}(\theta,\omega) \approx &-\left(\frac{1}{\gamma_A}\right)\sin\theta_A a_{VS} - \left[\left(\frac{1}{\gamma_A}\right)+\frac{1}{2}\right]\sin\theta_A a_\rho \\ &- 2\left(\frac{1}{\gamma_A}\right) Q_{S_0}^{-1} F_S(\omega)\sin\theta_A a_{QS}, \end{aligned} \tag{18}$$

for converted wave (P-S) reflection strengths, and

$$\begin{aligned} R^A_{\rm SS}(\phi,\omega) \approx &-\frac{1}{4}\left(1-7\sin^2\phi_A\right)a_{VS} - \frac{1}{2}\left(1-4\sin^2\phi_A\right)a_\rho \\ &- \frac{1}{2}Q_{S_0}^{-1}F_S(\omega)\left(1-7\sin^2\phi_A\right)a_{QS}, \end{aligned} \tag{19}$$

for S-S reflection strengths, where

$$\gamma_A = B^{-1} = \frac{V_{P_0}}{V_{S_0}}\frac{[1+Q_{S_0}^{-1}F_S(\omega)]}{[1+Q_{P_0}^{-1}F_P(\omega)]} \tag{20}$$

is the anelastic extension of the V_P/V_S ratio.

Elastic incidence medium

To produce the counterpart AVO approximations appropriate for an elastic (i.e., non-attenuating) incidence medium, we repeat the derivation above with some slight changes.

First, we define the quality factor perturbations differently:

$$a_{QP} = Q_{P_1}^{-1}, \quad a_{QS} = Q_{S_0}^{-1}. \tag{21}$$

Second, we re-define B, C and F to be consistent with infinite Q_P and Q_S in the incidence medium:

$$\begin{aligned} B &= \frac{V_{S_0}}{V_{P_0}}, \\ C &= \frac{V_{P_1}}{V_{P_0}}[1 + Q_{P_1}^{-1} F_P(\omega)]^{-1} \\ &\approx 1 + \frac{1}{2} a_{VP} - F_P(\omega) a_{QP}, \\ F &= \frac{V_{S_1}}{V_{S_0}}[1 + Q_{S_1}^{-1} F_S(\omega)]^{-1} \\ &\approx 1 + \frac{1}{2} a_{VS} - F_S(\omega) a_{QS}. \end{aligned} \tag{22}$$

Substituting these forms into the Zoeppritz equations above, and expanding the determinants in exactly the same way, we produce the alternative forms

$$\begin{aligned} R_{\text{PP}}^E(\theta, \omega) \approx & \frac{1}{4}(1 + \tan^2\theta) a_{VP} + \frac{1}{2}\left[1 - 4\left(\frac{V_{S_0}}{V_{P_0}}\right)^2 \sin^2\theta\right] a_\rho - 2\left(\frac{V_{S_0}}{V_{P_0}}\right)^2 \sin^2\theta a_{VS} \\ & - \frac{1}{2} F_P(\omega)\left(1 + \tan^2\theta\right) a_{QP} + 4\left(\frac{V_{S_0}}{V_{P_0}}\right)^2 F_S(\omega) \sin^2\theta a_{QS}, \end{aligned} \tag{23}$$

for P-P reflection strengths,

$$R_{\text{PS}}^E(\theta, \omega) \approx -\frac{V_{S_0}}{V_{P_0}} \sin\theta a_{VS} - \left(\frac{V_{S_0}}{V_{P_0}} + \frac{1}{2}\right) \sin\theta a_\rho + 2\frac{V_{S_0}}{V_{P_0}} F_S(\omega) \sin\theta a_{QS}, \tag{24}$$

for converted wave (P-S) reflection strengths, and

$$\begin{aligned} R_{\text{SS}}^E(\phi, \omega) \approx & -\frac{1}{4}\left(1 - 7\sin^2\phi\right) a_{VS} - \frac{1}{2}\left(1 - 4\sin^2\phi\right) a_\rho \\ & + \frac{1}{2} F_S(\omega)\left(1 - 7\sin^2\phi\right) a_{QS}, \end{aligned} \tag{25}$$

for S-S reflection strengths. The angles θ and ϕ are now real in precritical regimes, and the left-hand side angles and the right-hand side angles are, as in the purely elastic AVO approximations, real. Also, the reciprocal V_P/V_S ratio has reverted to its standard elastic form in the coefficients. We emphasize that the apparent similarity of these expressions to the anelastic incidence medium approximations above is partly illusory, as the perturbations are defined differently.

ANELASTIC AVO IN TERMS OF $\Delta Q_P/Q_P$ AND $\Delta Q_S/Q_S$

Starting with the core results of the previous section, we will now express each anelastic AVO approximations in two distinct ways, in terms of *relative changes*, and in terms of *reflectivities*. In elastic AVO the difference between these two quantities is minimal, since the relative changes in elastic properties are proportional to their corresponding elastic reflectivities. Not so in the anelastic case, because of the presence of dispersion.

So far our results have been expressed in terms of five dimensionless perturbations. Three are elastic: a_{VP}, a_{VS}, and a_ρ. The relative changes in P-wave velocity, S-wave velocity, and density are typically defined as

$$\begin{aligned}\frac{\Delta V_P}{V_P} &= 2\left(\frac{V_{P_1}-V_{P_0}}{V_{P_1}+V_{P_0}}\right)\\ \frac{\Delta V_S}{V_S} &= 2\left(\frac{V_{S_1}-V_{S_0}}{V_{S_1}+V_{S_0}}\right)\\ \frac{\Delta \rho}{\rho} &= 2\left(\frac{\rho_1-\rho_0}{\rho_1+\rho_0}\right)\end{aligned} \tag{26}$$

Given the definitions in equation (11), then, for small contrasts

$$\begin{aligned}\frac{\Delta V_P}{V_P} &\approx \frac{1}{2}a_{VP}\\ \frac{\Delta V_S}{V_S} &\approx \frac{1}{2}a_{VS}\\ \frac{\Delta \rho}{\rho} &\approx a_\rho.\end{aligned} \tag{27}$$

Hence to alter the approximations in the previous section to expressions in terms of the more familiar elastic relative changes, we simply substitute for a_{VP}, a_{VS}, and a_ρ using equation (27). For the two anelastic perturbations a_{QP} and a_{QS} things are not as straightforward: the forms depend on the type of incidence medium, and, as we have mentioned, on whether expression in terms of reflectivity or relative change is desired.

Anelastic incidence medium

Relative change

For anelastic AVO formulas in terms of *relative change* of V_P, V_S, ρ, and Q_P and Q_S across a boundary, the quantities $\Delta Q_P/Q_P$ and $\Delta Q_S/Q_S$ are defined in the same way as their elastic counterparts:

$$\begin{aligned}\frac{\Delta Q_P}{Q_P} &= 2\frac{Q_{P_1}-Q_{P_0}}{Q_{P_1}+Q_{P_0}}\\ \frac{\Delta Q_S}{Q_S} &= 2\frac{Q_{S_1}-Q_{S_0}}{Q_{S_1}+Q_{S_0}},\end{aligned} \tag{28}$$

in which case, using the definitions in equation (11), we may replace the perturbations in equations (17)–(19) with

$$\begin{aligned}\frac{\Delta Q_P}{Q_P} &\approx a_{QP} \\ \frac{\Delta Q_S}{Q_S} &\approx a_{QS},\end{aligned} \tag{29}$$

assuming $|a_{QP}|^2 \approx |a_{QS}|^2 \approx 0$. Equations (17)–(19) become

$$\begin{aligned}R^A_{\text{PP}}(\theta,\omega) \approx & \frac{1}{2}(1+\tan^2\theta_A)\frac{\Delta V_P}{V_P} + \frac{1}{2}\left[1 - 4\left(\frac{1}{\gamma_A}\right)^2 \sin^2\theta_A\right]\frac{\Delta\rho}{\rho} \\ & - 4\left(\frac{1}{\gamma_A}\right)^2 \sin^2\theta_A \frac{\Delta V_S}{V_S} + \frac{1}{2}Q_{P_0}^{-1}F_P(\omega)\left(1+\tan^2\theta_A\right)\frac{\Delta Q_P}{Q_P} \\ & - 4\left(\frac{1}{\gamma_A}\right)^2 Q_{S_0}^{-1}F_S(\omega)\sin^2\theta_A\frac{\Delta Q_S}{Q_S},\end{aligned} \tag{30}$$

for P-P reflection strengths,

$$\begin{aligned}R^A_{\text{PS}}(\theta,\omega) \approx & -2\left(\frac{1}{\gamma_A}\right)\sin\theta_A\frac{\Delta V_S}{V_S} - \left[\left(\frac{1}{\gamma_A}\right) + \frac{1}{2}\right]\sin\theta_A\frac{\Delta\rho}{\rho} \\ & - 2\left(\frac{1}{\gamma_A}\right)Q_{S_0}^{-1}F_S(\omega)\sin\theta_A\frac{\Delta Q_S}{Q_S},\end{aligned} \tag{31}$$

for converted wave (P-S) reflection strengths, and

$$\begin{aligned}R^A_{\text{SS}}(\phi,\omega) \approx & -\frac{1}{2}\left(1-7\sin^2\phi_A\right)\frac{\Delta V_S}{V_S} - \frac{1}{2}\left(1-4\sin^2\phi_A\right)\frac{\Delta\rho}{\rho} \\ & - \frac{1}{2}Q_{S_0}^{-1}F_S(\omega)\left(1-7\sin^2\phi_A\right)\frac{\Delta Q_S}{Q_S},\end{aligned} \tag{32}$$

for S-S reflection strengths. In Figures 3–5 the approximations in equations (30)–(32) are illustrated numerically. In Figure 3a the R^A_{PP} approximation of equation (30) in blue is plotted against the exact reflection coefficient in black. To illustrate the relative importance of including anelasticity at all (i.e., Q_P and Q_S), in Figure 3b the exact anelastic reflection coefficient (in black) is plotted against the exact reflection coefficient in the elastic limit (Q_P, $Q_S \to \infty$) with all other properties kept the same.

In Figure 4a the R^A_{PS} approximation of equation (31) in blue is plotted against the exact reflection coefficient in black. Again we illustrate the relative importance of including anelasticity in Figure 4b by plotting the exact anelastic reflection coefficient (in black) against the exact reflection coefficient in the elastic limit (Q_P, $Q_S \to \infty$) with all other properties kept the same.

Finally, in Figure 5a the R^A_{SS} approximation of equation (32) in blue is plotted against the exact reflection coefficient in black. Again we illustrate the relative importance of including anelasticity in Figure 5b by plotting the exact anelastic reflection coefficient (in black) against the exact reflection coefficient in the elastic limit (Q_P, $Q_S \to \infty$) with all other properties kept the same.

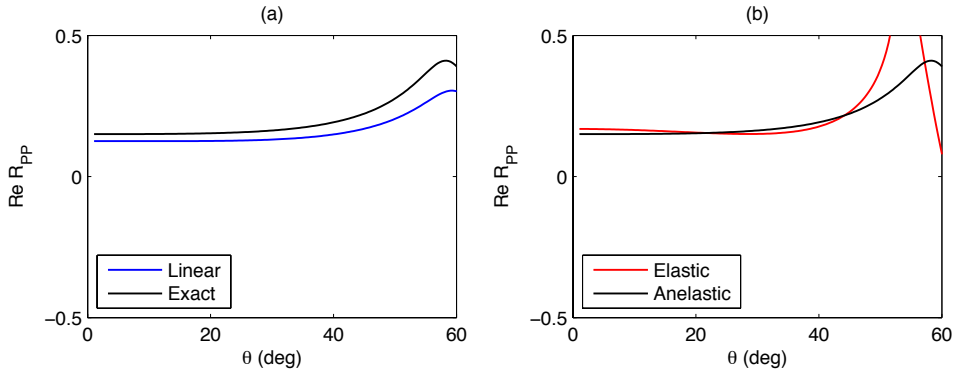

FIG. 3. R_{PP} approximation for anelastic incidence media in terms of the relative change in anelastic properties across the reflecting boundary. The parameters used are listed in Table 2. (a) Exact anelastic R_{PP} (black) vs. linear approximation (blue) as per equation (30). (b) Exact anelastic R_{PP} (black) vs. exact elastic R_{PP} (red) assuming entirely elastic media.

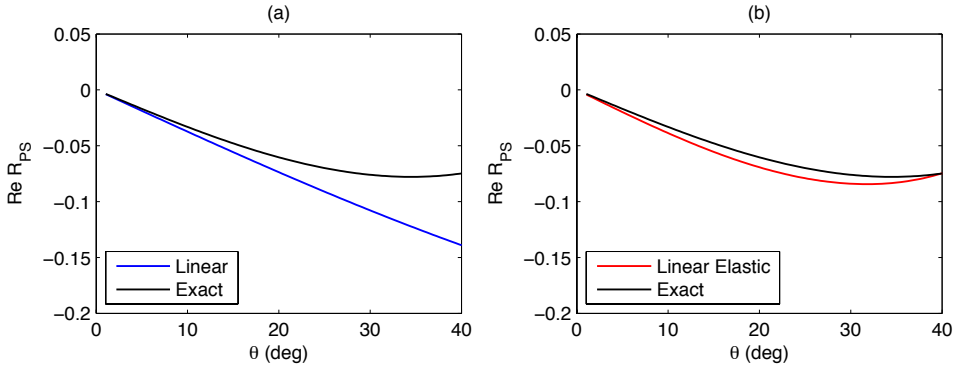

FIG. 4. R_{PS} approximation for anelastic incidence media in terms of the relative change in anelastic properties across the reflecting boundary. The parameters used are listed in Table 2. (a) Exact anelastic R_{PS} (black) vs. linear approximation (blue) as per equation (31). (b) Exact anelastic R_{PS} (black) vs. exact elastic R_{PS} (red) assuming entirely elastic media.

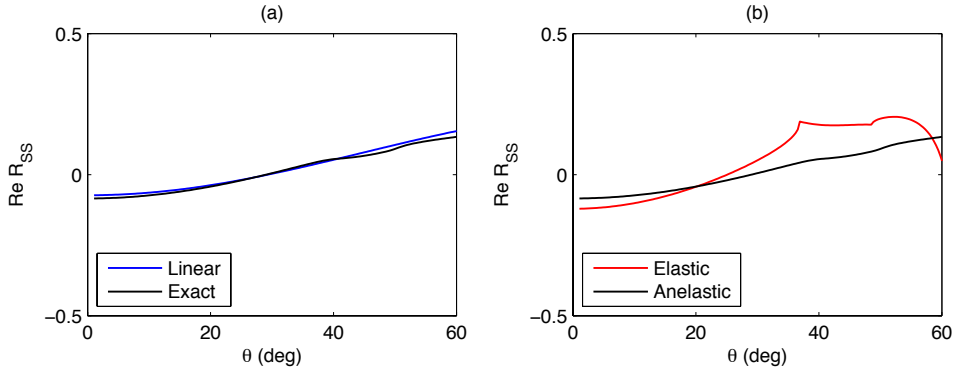

FIG. 5. R_{SS} approximation for anelastic incidence media in terms of the relative change in anelastic properties across the reflecting boundary. The parameters used are listed in Table 2. (a) Exact anelastic R_{SS} (black) vs. linear approximation (blue) as per equation (32). (b) Exact anelastic R_{SS} (black) vs. exact elastic R_{SS} (red) assuming entirely elastic media.

Reflectivity

The elastic relative change quantities are proportional to their counterpart elastic reflectivities. For instance, from equation (26) evidently

$$\frac{\Delta V_P}{V_P} = 2R_p, \tag{33}$$

where $R_p = R_{\rm PP}^{EE}(\theta = 0)$ is the P-wave reflectivity, for which $\rho_0 = \rho_1$ and $V_{S_0} = V_{S_1}$, that is, the normal incidence elastic reflection coefficient when there is no contrast in either density or S-wave velocity. Elastic AVO approximations can therefore be interpreted, with little additional manipulation, in terms of reflectivities.

The associated normal incidence Q_P and Q_S reflectivities are not as simple to relate to a_{QP} and a_{QS}, because the dispersion of anelastic media confers a frequency dependence on even normal-incidence reflection coefficients. In fact true Q_P and Q_S reflectivities are

$$\begin{aligned}\frac{\Delta Q_P}{Q_P} &= 2 \times \frac{F_P(\omega)\left(Q_{P_0}^{-1} - Q_{P_1}^{-1}\right)}{2 + F_P(\omega)\left(Q_{P_0}^{-1} - Q_{P_1}^{-1}\right)} \\ \frac{\Delta Q_S}{Q_S} &= -2 \times \frac{F_S(\omega)\left(Q_{S_0}^{-1} - Q_{S_1}^{-1}\right)}{2 + F_S(\omega)\left(Q_{S_0}^{-1} - Q_{S_1}^{-1}\right)},\end{aligned} \tag{34}$$

and they must replace not just a_{QP} and a_{QS} in equations (17)–(19), but all terms which contribute to frequency-dependent reflectivity, which includes the coefficients $Q_{P_0}^{-1}F_P(\omega)$ and $Q_{S_0}^{-1}F_S(\omega)$. We obtain

$$\begin{aligned}R_{\rm PP}^A(\theta,\omega) \approx & \frac{1}{2}(1+\tan^2\theta_A)\frac{\Delta V_P}{V_P} + \frac{1}{2}\left[1 - 4\left(\frac{1}{\gamma_A}\right)^2 \sin^2\theta_A\right]\frac{\Delta\rho}{\rho} \\ & - 4\left(\frac{1}{\gamma_A}\right)^2 \sin^2\theta_A \frac{\Delta V_S}{V_S} + \frac{1}{2}(1+\tan^2\theta_A)\frac{\Delta Q_P}{Q_P} \\ & + 4\left(\frac{1}{\gamma_A}\right)^2 \sin^2\theta_A \frac{\Delta Q_S}{Q_S},\end{aligned} \tag{35}$$

for P-P reflection strengths,

$$R_{\rm PS}^A(\theta,\omega) \approx -2\left(\frac{1}{\gamma_A}\right)\sin\theta_A\frac{\Delta V_S}{V_S} - \left[\left(\frac{1}{\gamma_A}\right) + \frac{1}{2}\right]\sin\theta_A\frac{\Delta\rho}{\rho} + 2\left(\frac{1}{\gamma_A}\right)\sin\theta_A\frac{\Delta Q_S}{Q_S}, \tag{36}$$

for converted wave (P-S) reflection strengths, and

$$\begin{aligned}R_{\rm SS}^A(\phi,\omega) \approx & -\frac{1}{2}\left(1 - 7\sin^2\phi_A\right)\frac{\Delta V_S}{V_S} - \frac{1}{2}\left(1 - 4\sin^2\phi_A\right)\frac{\Delta\rho}{\rho} \\ & + \frac{1}{2}\left(1 - 7\sin^2\phi_A\right)\frac{\Delta Q_S}{Q_S},\end{aligned} \tag{37}$$

for S-S reflection strengths. In Figures 6–8 the approximations in equations (35)–(37) are illustrated numerically. In Figure 6a the $R_{\rm PP}^A$ approximation of equation (30) in blue is plotted against the exact reflection coefficient in black. Again to illustrate the relative importance of including anelasticity, in Figure 6b the exact anelastic reflection coefficient (in black) is plotted against the exact reflection coefficient in the elastic limit (Q_P, $Q_S \rightarrow \infty$) with all other properties kept the same.

In Figure 7a the $R_{\rm PS}^A$ approximation of equation (31) in blue is plotted against the exact reflection coefficient in black. Again we illustrate the relative importance of including

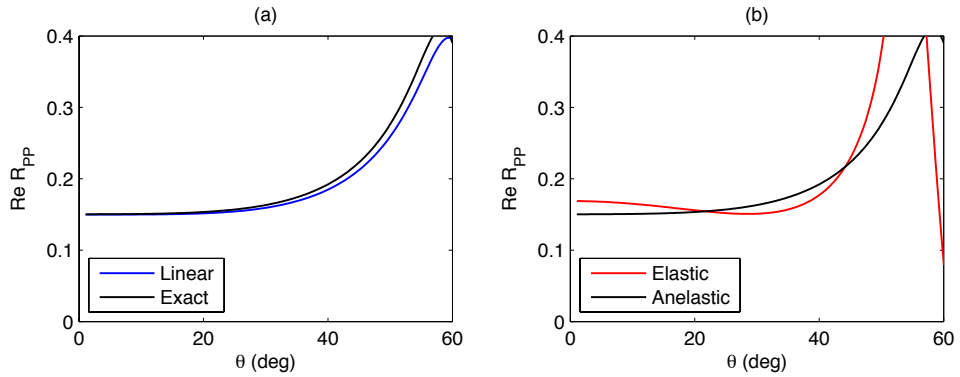

FIG. 6. R_{PP} approximation for anelastic incidence media in terms of the reflectivity at the reflecting boundary. The parameters used are listed in Table 2. (a) Exact anelastic R_{PP} (black) vs. linear approximation (blue) as per equation (35). (b) Exact anelastic R_{PP} (black) vs. exact elastic R_{PP} (red) assuming entirely elastic media.

anelasticity in Figure 7b by plotting the exact anelastic reflection coefficient (in black) against the exact reflection coefficient in the elastic limit (Q_P, $Q_S \rightarrow \infty$) with all other properties kept the same.

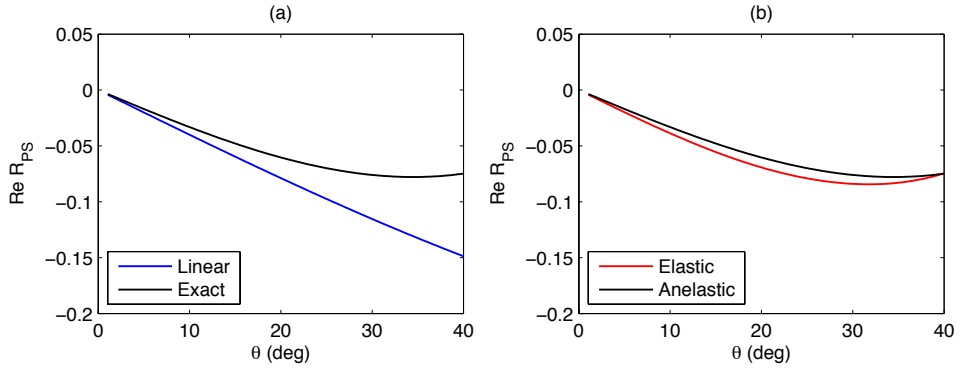

FIG. 7. R_{PS} approximation for anelastic incidence media in terms of the reflectivity at the reflecting boundary. The parameters used are listed in Table 2. (a) Exact anelastic R_{PS} (black) vs. linear approximation (blue) as per equation (36). (b) Exact anelastic R_{PS} (black) vs. exact elastic R_{PS} (red) assuming entirely elastic media.

Then, finally, in Figure 8a the R^A_{SS} approximation of equation (32) in blue is plotted against the exact reflection coefficient in black. Again we illustrate the relative importance of including anelasticity in Figure 8b by plotting the exact anelastic reflection coefficient (in black) against the exact reflection coefficient in the elastic limit (Q_P, $Q_S \rightarrow \infty$) with all other properties kept the same.

Elastic incidence medium

Relative change

When the incidence medium is elastic, the quality factors are infinite. This has meant that the perturbations a_{QP} and a_{QS} needed to be redefined in order for linear AVO approximations to be meaningfully expressed. It also means that posing AVO equations in terms of relative changes is at best a questionable enterprise. In this paper we choose to

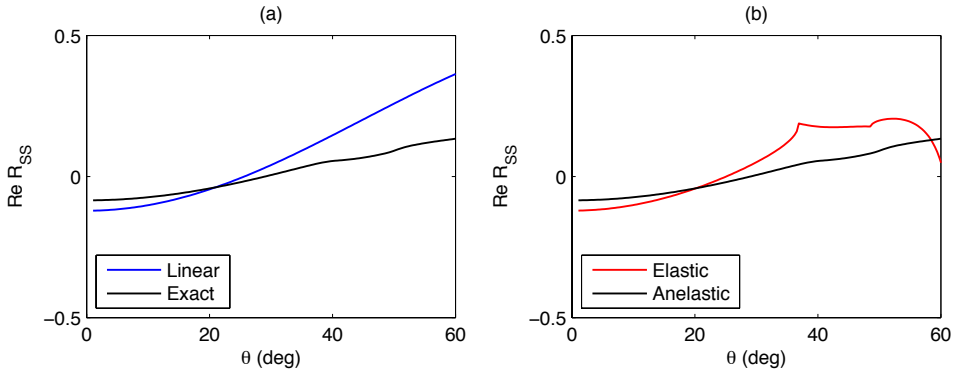

FIG. 8. R_{SS} approximation for anelastic incidence media in terms of the reflectivity at the reflecting boundary. The parameters used are listed in Table 2. (a) Exact anelastic R_{SS} (black) vs. linear approximation (blue) as per equation (37). (b) Exact anelastic R_{SS} (black) vs. exact elastic R_{SS} (red) assuming entirely elastic media.

view equations (23)–(25) themselves as the most convenient expressions for expressing anelastic AVO in terms of relative changes.

The numerical behaviour of equation (23), the linear approximation for R_{PP} in terms of relative change for an elastic incidence medium, is briefly illustrated in Figures 9a-b. In Figure 9a the red curve is the linear approximant to R_{PP}, plotted against the exact curve in black. In Figure 9b the same exact curve is plotted against the Aki-Richards approximation under the assumption of a purely elastic problem. The elastic/anelastic parameters used in the calculations are included in Table 2.

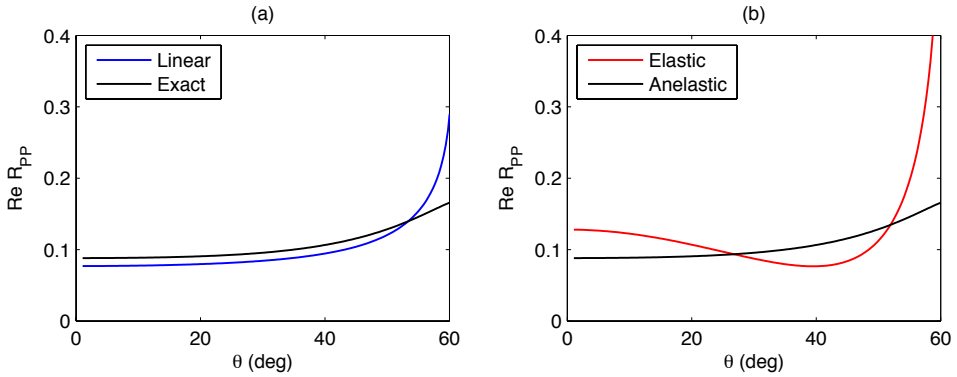

FIG. 9. R_{PP} approximation for elastic incidence media in terms of the relative change in anelastic parameters across the reflecting boundary. The parameters used are listed in Table 2. (a) Exact anelastic R_{PP} (black) vs. linear approximation (blue) as per equation (23). (b) Exact anelastic R_{PP} (black) vs. exact elastic R_{PP} (red) assuming entirely elastic media.

In Figures 10a-b the converted wave linear AVO approximation is similarly studied, using parameters listed in Table 2. The anelastic R_{PS} approximation which is (qualitatively) accurate out to $30 - 40°$.

Finally in Figures 11a-b we repeat this illustration for the R_{SS} dependence on incident S-wave angle ϕ, using the elastic and anelastic parameters listed in Table 2.

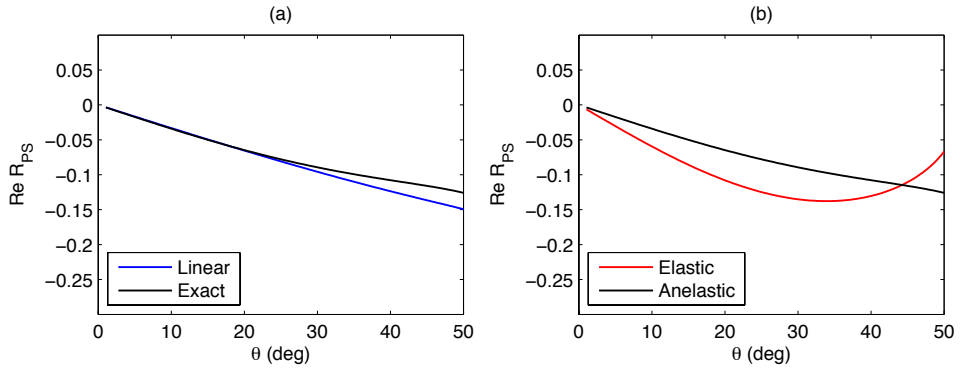

FIG. 10. R_{PS} approximation for elastic incidence media in terms of the relative change in anelastic parameters across the reflecting boundary. The parameters used are listed in Table 2. (a) Exact anelastic R_{PS} (black) vs. linear approximation (blue) as per equation (24). (b) Exact anelastic R_{PS} (black) vs. exact elastic R_{PS} (red) assuming entirely elastic media.

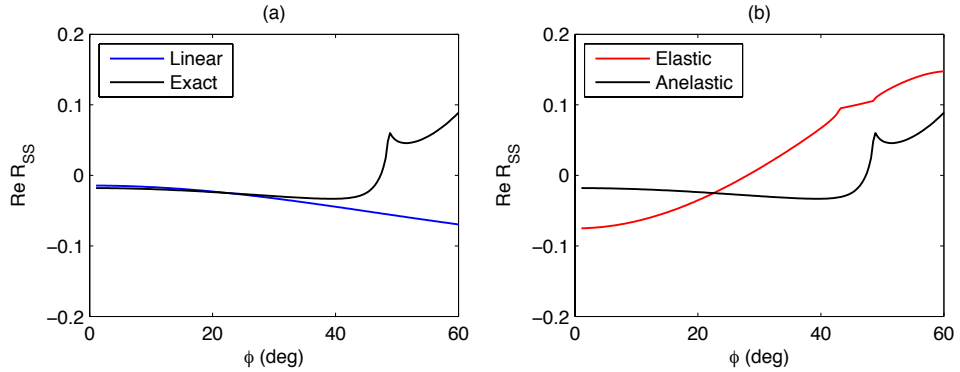

FIG. 11. R_{SS} approximation for elastic incidence media in terms of the relative change in anelastic parameters across the reflecting boundary. The parameters used are listed in Table 2. (a) Exact anelastic R_{SS} (black) vs. linear approximation (blue) as per equation (25). (b) Exact anelastic R_{SS} (black) vs. exact elastic R_{SS} (red) assuming entirely elastic media.

Reflectivity

It is not difficult to re-write anelastic AVO for elastic incidence media in terms of reflectivities, for contrasts from infinite to finite Q only are seen numerically and in laboratory studies to cause definite reflections (Lines et al., 2012). The reflectivities are

$$\begin{aligned}\frac{\Delta Q_P}{Q_P} &= -2 \times \frac{F_P(\omega) Q_{P_1}^{-1}}{2 - F_P(\omega) Q_{P_1}^{-1}} \\ \frac{\Delta Q_S}{Q_S} &= 2 \times \frac{F_S(\omega) Q_{S_1}^{-1}}{2 - F_S(\omega) Q_{S_1}^{-1}},\end{aligned} \tag{38}$$

and these, when substituted (for all terms which contribute to normal incidence reflection strengths) into the original forms in equations (23)–(25), provide the formulas

$$\begin{aligned} R^E_{\rm PP}(\theta,\omega) \approx & \frac{1}{2}(1+\tan^2\theta)\frac{\Delta V_P}{V_P} + \frac{1}{2}\left[1-4\left(\frac{V_{S_0}}{V_{P_0}}\right)^2\sin^2\theta\right]\frac{\Delta\rho}{\rho} \\ & - 4\left(\frac{V_{S_0}}{V_{P_0}}\right)^2\sin^2\theta\frac{\Delta V_S}{V_S} + \frac{1}{2}(1+\tan^2\theta)\frac{\Delta Q_P}{Q_P} \\ & + 4\left(\frac{V_{S_0}}{V_{P_0}}\right)^2\sin^2\theta\frac{\Delta Q_S}{Q_S}, \end{aligned} \tag{39}$$

for P-P reflection strengths,

$$R^E_{\rm PS}(\theta,\omega) \approx -2\frac{V_{S_0}}{V_{P_0}}\sin\theta\frac{\Delta V_S}{V_S} - \left(\frac{V_{S_0}}{V_{P_0}}+\frac{1}{2}\right)\sin\theta\frac{\Delta\rho}{\rho} + 2\frac{V_{S_0}}{V_{P_0}}\sin\theta\frac{\Delta Q_S}{Q_S}, \tag{40}$$

for converted wave (P-S) reflection strengths, and

$$\begin{aligned} R^E_{\rm SS}(\phi,\omega) \approx & -\frac{1}{2}\left(1-7\sin^2\phi\right)\frac{\Delta V_S}{V_S} - \frac{1}{2}\left(1-4\sin^2\phi\right)\frac{\Delta\rho}{\rho} \\ & + \frac{1}{2}\left(1-7\sin^2\phi\right)\frac{\Delta Q_S}{Q_S}, \end{aligned} \tag{41}$$

for S-S reflection strengths. In Figures 12–14 the approximations in equations (39)–(41) are illustrated numerically. In Figure 6a the $R^E_{\rm PP}$ approximation of equation (30) in blue is plotted against the exact reflection coefficient in black. Again to illustrate the relative importance of including anelasticity, in Figure 6b the exact anelastic reflection coefficient (in black) is plotted against the exact reflection coefficient in the elastic limit (Q_P, $Q_S \rightarrow \infty$) with all other properties kept the same.

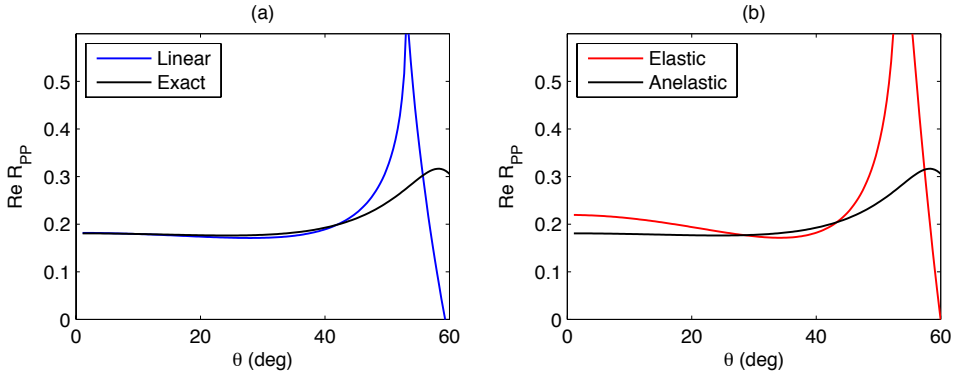

FIG. 12. $R_{\rm PP}$ approximation for elastic incidence media in terms of the reflectivity at the reflecting boundary. The parameters used are listed in Table 2. (a) Exact anelastic $R_{\rm PP}$ (black) vs. linear approximation (blue) as per equation (39). (b) Exact anelastic $R_{\rm PP}$ (black) vs. exact elastic $R_{\rm PP}$ (red) assuming entirely elastic media.

In Figure 13a the $R^E_{\rm PS}$ approximation of equation (40) in blue is plotted against the exact reflection coefficient in black. Again we illustrate the relative importance of including anelasticity in Figure 13b by plotting the exact anelastic reflection coefficient (in black)

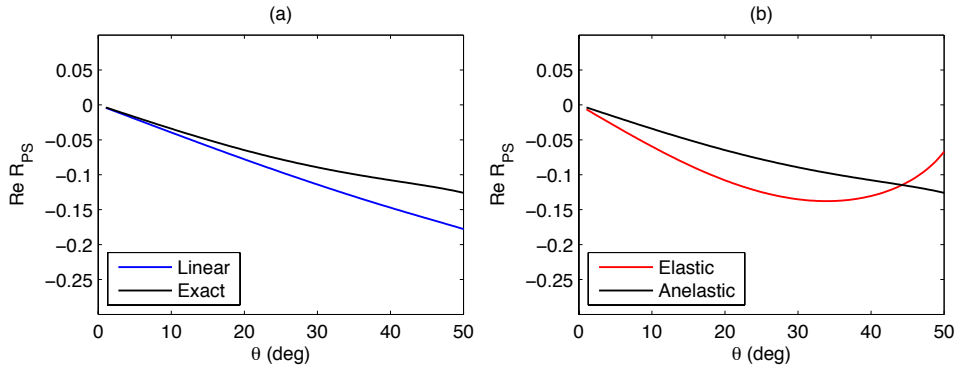

FIG. 13. $R_{\rm PS}$ approximation for elastic incidence media in terms of the reflectivity at the reflecting boundary. The parameters used are listed in Table 2. (a) Exact anelastic $R_{\rm PS}$ (black) vs. linear approximation (blue) as per equation (40). (b) Exact anelastic $R_{\rm PS}$ (black) vs. exact elastic $R_{\rm PS}$ (red) assuming entirely elastic media.

against the exact reflection coefficient in the elastic limit (Q_P, $Q_S \rightarrow \infty$) with all other properties kept the same.

In Figure 14a the $R^E_{\rm SS}$ approximation of equation (41) in blue is plotted against the exact reflection coefficient in black. Again we illustrate the relative importance of including anelasticity in Figure 14b by plotting the exact anelastic reflection coefficient (in black) against the exact reflection coefficient in the elastic limit (Q_P, $Q_S \rightarrow \infty$) with all other properties kept the same.

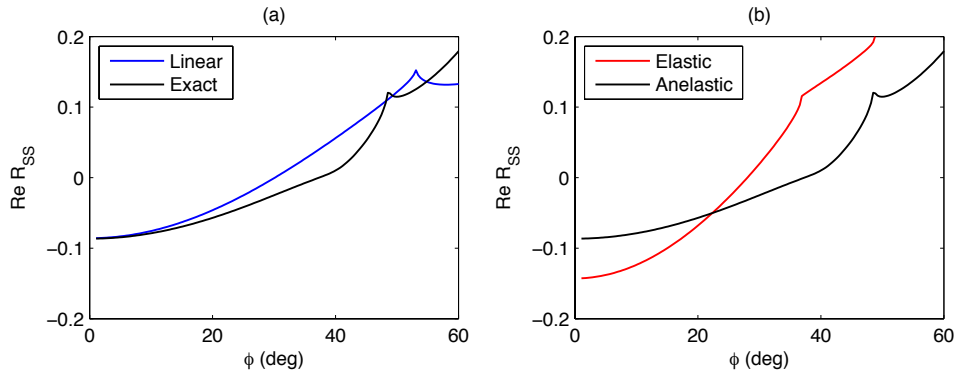

FIG. 14. $R_{\rm SS}$ approximation for elastic incidence media in terms of the reflectivity at the reflecting boundary. The parameters used are listed in Table 2. (a) Exact anelastic $R_{\rm SS}$ (black) vs. linear approximation (blue) as per equation (41). (b) Exact anelastic $R_{\rm SS}$ (black) vs. exact elastic $R_{\rm SS}$ (red) assuming entirely elastic media.

CONCLUSIONS

We have presented twelve formulas for the approximation of anelastic reflection coefficients: $R_{\rm PP}$, $R_{\rm PS}$, and $R_{\rm SS}$ for every combination of anelastic and elastic incidence media, and relative change- vs. reflectivity-type perturbations. Each has been illustrated for a single set of anelastic parameters, and compared against both its exact counterpart and its exact elastic counterpart. The latter is a rough indication of whether the "trouble" of accounting approximately for anelasticity in AVO is "worth the effort". Albeit via (i) examination of a single example, and (ii) qualitative analysis, we can come to some conclusions about which

Approximation type	Equations	R_{PP}	R_{PS}	R_{SS}
Anelastic incidence, relative change	30–32	$\sim$	$\times$	✓
Anelastic incidence, reflectivity	35–37	✓	$\times$	$\sim$
Elastic incidence, relative change	23–25	✓	✓	✓
Elastic incidence, reflectivity	39–41	✓	✓	✓

Table 3. Relative accuracy of linearized anelastic reflection coefficient approximations. Symbols: ✓: anelastic linear approximation is more accurate than an exact elastic calculation; $\times$ anelastic linear approximation is less accurate than an exact elastic calculation; $\sim$ difference is not visually obvious.

approximations are worth our time.

In Table 3, the formulas are evaluated with a ✓, a $\sim$, or a $\times$, depending on whether a visual comparison of the elastic reflection coefficient (what you would get if you ignored anelasticity in your AVO modeling) and the anelastic approximation revealed that the anelastic formula added value, made no difference, or was worse, respectively.

The two instances in which the judgment was "worse" (which were both for the converted wave reflection coefficient), are traceable to the linearity of the approximations, and not specifically to the inclusion of Q_P and Q_S. Nevertheless, the anelastic converted wave approximation was seen to add value only for the case of an elastic incidence medium, and thus merits some care in application. In most cases, there is clear uptick in accuracy in the anelastic approximations: even in the two cases in which the judgment was $\sim$, the trends if not the magnitudes of the approximations tended to be an improvement over the elastic limit.

ACKNOWLEDGMENTS

This work was funded by the CREWES project. CREWES sponsors and research personnel are thanked.

REFERENCES

Aki, K., and Richards, P. G., 2002, Quantitative Seismology: University Science Books, 2nd edn.

Castagna, J. P., and Backus, M., 1993, Offset-dependent reflectivity: theory and practice of AVO analysis: SEG.

Chapman, M., Liu, E., and Li, X. Y., 2006, The influence of fluid-sensitive dispersion and attenuation on AVO analysis: Geophysical Journal International, **167**, No. 1, 89–105.

Foster, D. J., Keys, R. G., and Lane, F. D., 2010, Intepretation of AVO anomalies: Geophysics, **75**, 75A3–75A13.

Innanen, K. A., 2011, Inversion of the seismic AVF/AVA signatures of highly attenuative targets: Geophysics, **76**, No. 1, R1–R11.

Innanen, K. A., 2012, Coupling in AVO and the Wiggins approximation: Submitted to Geophysics.

Lines, L. R., Innanen, K. A., Vasheghani, F., Wong, J., Sondergeld, C., Treitel, S., and Ulrych, T. J., 2012, Experimental confirmation of "Reflections on Q": SEG Expanded Abstracts, **31**.

Odebeatu, E., Zhang, J., Chapman, M., Liu, E., and Li, X. Y., 2006, Application of spectral decomposition to detection of dispersion anomalies associated with gas saturation: The Leading Edge, **2**, 206–210.

Quintal, B., Schmalholz, S. M., and Podladchikov, Y. Y., 2009, Low-frequency reflections from a thin layer with high attenuation caused by interlayer flow: Geophysics, **74**, N15–N23.

Shuey, R., 1985, A simplification of the Zoeppritz equations: Geophysics, **50**, 609–614.